THE JOURNAL OF BIOLOGICAL CHEMISTRY VOL. 283, NO. 17, pp. 11763–11771, April 25, 2008

Dynamic Interaction of the Measles Virus Hemagglutinin with Its Receptor Signaling Lymphocytic Activation Molecule (SLAM, CD150)*[S]

Received for publication, February 4, 2008, and in revised form, February 19, 2008 Published, JBC Papers in Press, February 21, 2008, DOI 10.1074/jbc.M800896200

Chanakha K. Navaratnarajah[‡], Sompong Vongpunsawad[‡], Numan Oezguen[§], Thilo Stehle[¶], Werner Braun[§], Takao Hashiguchi[‖], Katsumi Maenaka[**], Yusuke Yanagi[‖], and Roberto Cattaneo[‡1]

*From the [‡]Department of Molecular Medicine and Virology and Gene Therapy Graduate Track, Mayo Clinic, Rochester, Minnesota 55905, the [§]Sealy Center for Structural Biology, University of Texas Medical Branch, Galveston, Texas 77555, the [¶]Interfakultäres Institut für Biochemie, University of Tübingen, D-72076 Tübingen, Germany and Vanderbilt University School of Medicine, Nashville, Tennessee 37240, and the [‖]Department of Virology, Faculty of Medicine and the **Division of Structural Biology, Medical Institute of Bioregulation, Kyushu University, Fukuoka 812-8582, Japan*

The interaction of measles virus with its receptor signaling lymphocytic activation molecule (SLAM) controls cell entry and governs tropism. We predicted potential interface areas of the measles virus attachment protein hemagglutinin to begin the investigation. We then assessed the relevance of individual amino acids located in these areas for SLAM-binding and SLAM-dependent membrane fusion, as measured by surface plasmon resonance and receptor-specific fusion assays, respectively. These studies identified one hemagglutinin protein residue, isoleucine 194, which is essential for primary binding. The crystal structure of the hemagglutinin-protein localizes Ile-194 at the interface of propeller blades 5 and 6, and our data indicate that a small aliphatic side chain of residue 194 stabilizes a protein conformation conducive to binding. In contrast, a quartet of residues previously shown to sustain SLAM-dependent fusion is not involved in binding. Instead, our data prove that after binding, this quartet of residues on propeller blade 5 conducts conformational changes that are receptor-specific. Our study sets a structure-based stage for understanding how the SLAM-elicited conformational changes travel through the H-protein ectodomain before triggering fusion protein unfolding and membrane fusion.

Measles is a leading cause of childhood morbidity and mortality in developing countries (1). The immune suppression that accompanies infection with wild-type measles viruses (MV)[2] exposes individuals to secondary infections causing most of the fatalities associated with the disease (2). Live attenuated MV vaccines have effectively reduced the morbidity and mortality of measles world-wide (3). The difference in pathology between the wild-type and vaccine strains is in part explained by the receptors used for cell entry. Wild-type MV uses the signaling lymphocyte activation molecule (SLAM, CD150) (4–7), while the vaccine strain has gained the ability to also use the ubiquitous protein CD46 (8–10). SLAM-targeting accounts for lymphotropism and is central to understanding MV tropism and disease progression.

Receptor attachment of MV and the other morbilliviruses is mediated by hemagglutinin (H) homodimers. Unlike other members of the *Paramyxoviridae*, the morbillivirus H-proteins do not have neuraminidase activity. Upon receptor attachment, H induces conformational changes in the trimeric fusion (F) protein, resulting in the fusion of viral and cellular membranes (11, 12). MV H is a 617-amino acid type II transmembrane glycoprotein, which is comprised of an N-terminal cytoplasmic tail, a membrane-spanning domain, and an extracellular stalk region connected to a C-terminal globular head (13).

Previously, we generated a three-dimensional model of the extracellular domain of the MV H-protein based on the crystal structure of Newcastle Disease Virus (NDV) HN (hemagglutinin neuraminidase) protein (sequence identity of 12%), a related paramyxovirus (14, 15). This model predicts that the MV H ectodomain has a 6-blade propeller structure. We previously localized several residues specific for SLAM- or CD46-dependent fusion onto the H-protein model. Seven amino acids important for SLAM- and nine for CD46-dependent fusion function were located in contiguous areas in β-sheet 5 and 4, respectively. Especially interesting were four residues essential for SLAM-dependent fusion-support, amino acids Tyr-529, Asp-530, Arg-533, and Tyr-553, to be named the β-sheet 5 quartet (bs-5 quartet).

To further characterize the mechanism of interaction of the MV H-protein with its receptor, SLAM, we extended H mutagenesis based on a suite of programs that allow the prediction of potential interacting surfaces. The prediction was based on the detailed analysis of sequence conservation in homologues of MV H by stereophysicochemical variability plots

* This work was supported in part by Grant R01 CA090363 from the National Institutes of Health and the Mayo Foundation. The costs of publication of this article were defrayed in part by the payment of page charges. This article must therefore be hereby marked "*advertisement*" in accordance with 18 U.S.C. Section 1734 solely to indicate this fact.

[S] The on-line version of this article (available at http://www.jbc.org) contains supplemental data and Fig. S1.

[1] To whom correspondence should be addressed: 200 1st St. SW, Guggenheim 1838, Rochester MN 55905. Tel.: 507-538-1188; Fax: 507-266-2122; E-mail: cattaneo.roberto@mayo.edu.

[2] The abbreviations used are: MV, measles virus; SLAM , signaling lymphocyte activation molecule; H, hemagglutinin; F, fusion protein; NDV, Newcastle Disease Virus; HN, hemagglutinin neuraminidase; SVP, stereophysicochemical variability plots; SPR, surface plasmon resonance; DMEM, Dulbecco's modified Eagle's medium; FBS, fetal bovine serum; MOI, multiplicity of infection; CHO, chinese hamster ovary cells; FACS, fluorescent-activated cell sorting; TCID, tissue culture infective dose.

(SVP) and a recently developed computational method named InterProSurf (16). A final assessment of potential receptor binding areas relied upon the combined predictions of InterProSurf and SVP. Screening of the library of H-protein mutants was based on a receptor-specific cell-to-cell fusion assay, and identified Ile-194 as a residue critical for SLAM-dependent fusion-support. A surface plasmon resonance (SPR) assay discriminated between residues involved in primary receptor binding, and those sustaining H-protein conformational changes subsequent to binding. The binding kinetics revealed that the Ile-194 mutations ablated SLAM binding, whereas the bs-5 quartet residues are involved in a post-binding event.

EXPERIMENTAL PROCEDURES

Cells and Viruses—B95a, an Epstein-Barr virus-transformed marmoset B lymphoblastoid cell line (kindly provided by D. Gerlier), and Vero (African green monkey kidney) cells were maintained in Dulbecco modified Eagle's medium (DMEM) supplemented with 10 and 5% fetal bovine serum (FBS), respectively. CHO-SLAM (Chinese hamster ovary cells expressing human SLAM) cells were maintained in RPMI 1640 medium supplemented with 10% FBS and 0.5 mg/ml of G418. The DF-1 chicken cell line was maintained in DMEM supplemented with 10% FBS at 39 °C. The rescue helper cell line 293-3-46 (17) was grown in DMEM with 10% FBS and 1.2 mg/ml of G418.

Prediction of Interaction Surface Regions with InterProSurf—Given a three-dimensional structure (either an experimental structure or a theoretical model) InterProSurf (18) calculates for each surface residue propensities for having this residue in a protein-protein interface region. In a second step, it clusters high scoring residues together and reports these clusters to the user.

Structure Modelling—A more advanced model of the MV H-protein, which was used to guide late phases of mutagenesis, is described under supplemental materials.

Plasmids, Mutagenesis, and Receptor-specific Cell-to-Cell Fusion Assay—All H-protein mutants were generated in the pCG-H plasmid (19) by the QuikChange site-directed mutagenesis (Stratagene). The integrity of the clone was confirmed by sequencing the H-protein gene in the vicinity of the mutation. For the cell-based fusion assay, Vero cells or CHO-SLAM cells were plated on 24-well tissue culture plates without antibiotics and allowed to reach 80% confluence prior to transfection. Equal amounts (1 μg) of the envelope protein expression plasmids, pCG-F (19) and pCG-H were transfected into the cells using Lipofectamine 2000 (Invitrogen) according to the manufacturer's instructions. In brief, 2 μl of Lipofectamine 2000 was mixed with 50 μl of Opti-MEM I reduced-serum medium (Opti-MEM, Invitrogen) and incubated at room temperature for 5 min. Appropriate volumes of pCG-H and pCG-F plasmid DNAs were also diluted in 50 μl of Opti-MEM, and the Lipofectamine- and DNA-containing solutions were mixed and incubated for 20 min prior to addition to cells. Cells were analyzed and the fusion effect quantified 36-h post-transfection. The extent of fusion was recorded using the following convention: 0 (empty bars/rectangles), no syncytium formation; + (partially filled), syncytia found on some fields of view; ++ (partially filled), syncytia found in most fields of view; and +++ (completely filled), the majority of the cells were in syncytia. Fusion scores are based on the average of three independent experiments.

Rescue of Recombinant Viruses—Infectious MV genomes containing selected mutations in the H-protein sequence were generated by subcloning the PacI/SpeI fragment containing the H open reading frame from pCG-H into the similarly digested p(+)MVeGFP plasmid. This MV genome has an enhanced green fluorescent protein sequence inserted in an additional transcription unit located upstream of the N gene (20). All the MV genomes generated were of hexameric length and were rescued as described previously (17, 21). Virus stocks were prepared by infecting Vero cells at an MOI of 0.01 and then incubated at 37 °C until a majority of the cells were in syncytia. At this point cells were harvested in Opti-MEM and freeze-thawed once. Titers were determined by 50% tissue culture infective dose titration ($TCID_{50}$) on Vero cells. To compare the infectivity of recombinant viruses, cells were washed with phosphate-buffered saline (PBS) and infected at an MOI of 0.l in Opti-MEM for 2 h at 37 °C. The extent of the infection was recorded by fluorescence microscopy at 36-h post-infection.

Soluble Hemagglutinin (sH) Expression—The ectodomain of the H-protein (sH) comprising residues 60–617 was cloned in-frame with the murine Ig κ-chain leader sequence and a FLAG epitope, and this construct was placed in a pCG vector containing the zeocin-resistance gene. The sH expression vector, pCG-sH-IRES-Zeo and its derivatives containing mutations in the H-coding sequence were transfected into CHO K1 cells using Lipofectamine 2000 according to the manufacturer's instructions (Invitrogen). Stable clones were isolated under zeocin selection. CHO K1 cells stably expressing the H-protein of interest were grown in serum-free medium for 24 h. The cell supernatant was harvested and filtered through a 0.45-μm pore size filter, concentrated using 30-kDa size exclusion Centricon columns (Millipore), and buffer-exchanged with HEPES buffer (10 mM HEPES, 150 mM NaCl, pH 7.5). sH proteins were analyzed by immunoblot and found to have an electrophoretic mobility under reducing conditions consistent with their size (data not shown). The sizes of all the sH proteins were about two times higher under nonreducing conditions compared with reducing conditions, indicating the formation of disulfide-linked dimers. We were unable to express and purify useful amounts of the wild-type IC-B strain sH-protein without the N481Y mutation.

Soluble Receptors—The extracellular domain of CD46 consisting of the first 303 amino acids of CD46 (complement control protein motifs 1–4) was fused to amino acids 96–323 of the constant region of rabbit IgG gene, which is part of the retroviral vector RCASBP (a kind gift of M. Federspiel) (22). RCASBP (5 μg) was transfected into DF-1 cells by the calcium phosphate precipitation method (Promega). Cell supernatant containing soluble CD46 was harvested 3–5 days post-transfection. Supernatants were filtered through a 0.2-μm membrane and sent to Mayo's Protein Core Facility for purification using affinity column chromatography with protein G (GE Healthcare). sCD46 was eluted with 25 mM diethylamine, pH 11.4 and buffer-exchanged with PBS. The size and purity of sCD46 was verified by SDS-PAGE analysis. For sSLAM expression, residues 21–230 of

the SLAM precursor protein (extracellular region) were expressed fused to human IgG1-Fc to allow for purification by protein A affinity chromatography from cell culture supernatant. CHO Lec 3.2.8.1 (23) cells were used for expression. Thrombin was used to release the SLAM ectodomain and then purified to homogeneity by gel filtration using a Superdex 200 column (GE Healthcare).

Receptor Binding Kinetics of MV H-protein—The interaction of the MV H-protein with sCD46 and sSLAM was monitored by SPR using a BIAcore 3000 instrument and CM5 sensor chips (GE Healthcare). HBS buffer (10 mM HEPES, 250 mM NaCl, pH 7.4) was used for all protein dilutions and as the running buffer. To attach the MV H-protein to the sensor chip surface, first the anti-FLAG antibody (Sigma) was immobilized onto the chip surface using the amine coupling kit (GE Healthcare). Anti-FLAG (30 μg/ml) was diluted in 10 mM sodium acetate, pH 5.5 and ~10,000 resonance units were immobilized on the chip surface. Next, the MV H-protein was injected over the anti-FLAG antibody at 10 μl/min for 5 min to capture the H-protein to the sensor chip surface. To monitor receptor binding, different concentrations of sCD46 and sSLAM (0.1 μM-1 μM) were injected over the captured MV H-proteins at 25 μl/min. The soluble receptors were then injected over the CM5 sensor chip surfaces either exhibiting or lacking captured sH-protein. The surfaces lacking captured sH served as control surfaces for nonspecific receptor binding. The antibody surface was regenerated by injection of 50 mM citric acid, pH 3.0 for 60 s followed by 10 mM glycine, pH 3.0 for 60 s with no change in the activity of the monoclonal antibody surface monitored. The curve-fitting function of the BIAevaluation 4.1 software was used to fit rate equations derived from the simple 1:1 Langmuir binding model to the experimental data. The affinity dissociation constant (K_d) was determined either from the kinetic rate constants or derived from Scatchard analysis of steady-state conditions.

Virus Cell Binding Assay—For virus purification, Vero cells (two 15-cm tissue culture dishes) were infected at an MOI of 0.1 and incubated at 37 °C until ~90% of the cells were in syncytia. At this point, the cells were scraped in Opti-MEM and subjected to a single freeze-thaw cycle. The cell extracts were clarified by centrifugation at 15,000 × *g* for 10 min. The clarified cell extract was layered over a 20–60% discontinuous sucrose gradient and centrifuged at 112,000 × *g* for 2 h at 4 °C. The virus band was harvested at the interphase between the two layers. Edmonston B-based parental MV particles, and the recombinant derivative containing the I194S mutation were used for the binding assays. B95a cells were detached from tissue culture plates by PBS-EDTA treatment. About 2×10^5 cells were incubated with ~7.35×10^4 $TCID_{50}$/cell purified MV particles at 4 °C for 1.5 h in DMEM supplemented with 5% FBS and 0.03% NaN_3. Cells were washed three times with PBS supplemented with 5% FBS, 0.0005% Tween 20, and 0.03% NaN_3. Virus bound to cells was detected by staining cells with an anti-H monoclonal antibody (MAB8905, Millipore) followed by a secondary PE-conjugated antibody for 1 h each. Cells were fixed overnight in 2% paraformaldehyde prior to FACS analysis on a FACScan instrument (Becton Dickinson).

RESULTS

Prediction of H-protein Potential Interface Areas and Their Mutagenesis—To identify additional residues involved in receptor-dependent fusion-support we subjected the MV H three-dimensional model to InterProSurf analysis (15, 18). InterProSurf, which identifies clusters of residues available for interaction with another protein, successfully predicted interacting surfaces of the E1 envelope protein of Venezuelan equine encephalitis virus and the capsid protein of human hepatitis B virus (16, 24). The program divides the solvent accessible surface of proteins in 32 clusters and calculates a score for each cluster as being part of an interacting surface. It has been empirically determined that the first 8–10 high scoring clusters provide a good balance for the prediction quality (16).

Additional information on the location of important functional residues on the surface of the H-protein was provided by SVPs. SVPs project the positional variability of physical chemical properties of amino acids in a multiple alignment of protein sequences onto a three-dimensional structure (16, 25). We assumed that the H-proteins of all morbilliviruses recognize their receptors by a similar mechanism, and hypothesized that surface-exposed residues that are part of the receptor binding sites are quantitatively more conserved in their physical chemical properties than residues outside of these binding sites and SVPs were used to map this information onto the three-dimensional model of H.

83 residues were predicted by InterProSurf to be solvent accessible and to be part of an interacting surface. These residues are highlighted in color in Fig. 1*A*. Three residues, Phe-552, Tyr-553, and Pro-554 (*red shading*), were previously shown to be important for SLAM-dependent fusion (15). Residues Ala-428, Phe-431, Leu-464, and Tyr-481 (*blue shading* where visible) are important for CD46-dependent fusion (26–28). Twelve other residues had already been mutated and found not to be important for fusion-support (data not shown).

The remaining 64 candidate residues (*green shading*) were mutated. To limit protein folding and transport defects, two small amino acids were selected: alanine to replace charged and polar residues, and serine to substitute for apolar residues. The mutations are shown in Fig. 1*B*, where the location and identity of the substitution is indicated above the original MV H-protein sequence. A set of 40 mutants were made in blocks of 2–3 (linearly) contiguous amino acids, or single residues when no contiguous blocks were predicted. Subsequently, single mutations were made within relevant blocks. The cDNAs were checked for integrity around the site of mutagenesis, and at least two independent clones were tested for each mutant.

Isoleucine 194 Is Necessary for SLAM-dependent Fusion-Support—The mutated H-proteins were then tested for fusion-support capacity in receptor-specific cell fusion assays based on co-expression of the standard F-protein. The cell fusion assays were conducted in rodent cells stably expressing SLAM but not CD46 (CHO-SLAM cells) or in Vero cells, a simian cell line which naturally expresses CD46 but not SLAM. A semi-quantitative assessment of the fusion-support capacity of the mutant H-proteins is shown in Fig. 1*C*.

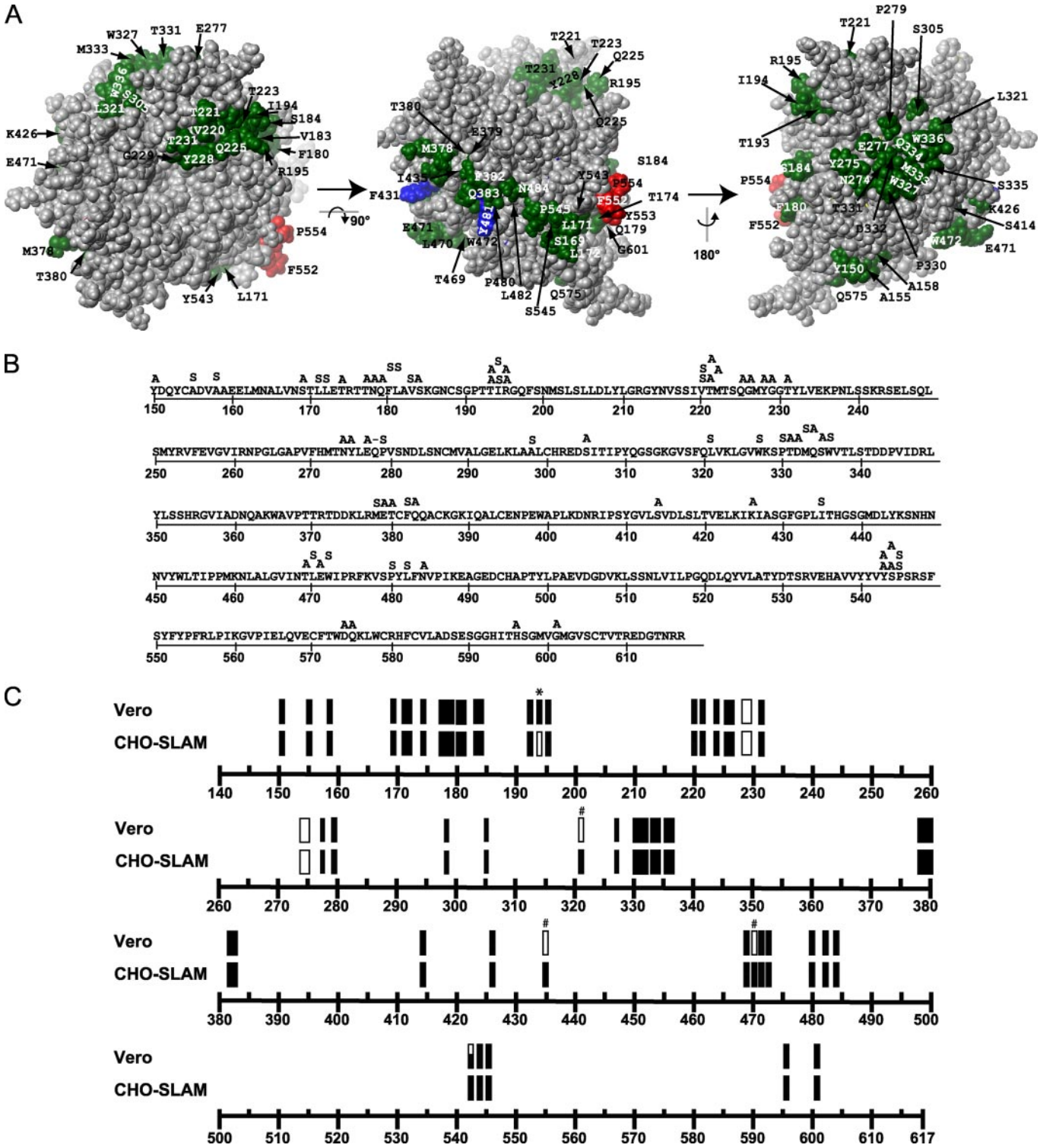

FIGURE 1. **Mutagenesis of predicted interaction regions of MV H.** *A*, MV H model, with residues predicted to be part of protein-protein interactions depicted in *red* (SLAM-specific residues), *blue* (CD46-specific residues), and *green* (residues mutated in this study). The *left panel* is a view of the protein from the top; in the *center panel* the model was rotated 90° around the *x*-axis; the *right panel* was generated by rotating the center model 180° around the *y*-axis. The molecule has been depth-cued using the fog function to give perspective. *B*, MV H sequence and the mutations introduced. Single and multiple amino acid substitutions are indicated above the sequence. Alanine (*A*) was used to replace charged and polar residues and serine (*S*) was used to replace apolar residues. *C*, fusion efficiency of the H-protein mutants in Vero or CHO-SLAM cells. *Rectangles* represent multiple amino acid substitutions; *bars* represent single amino acid substitutions. *Filled objects* indicate full fusion activity, *void objects* indicate lack of fusion activity, and *partially filled objects* indicate intermediate fusion levels as defined under "Experimental Procedures." Single amino acid substitutions that are SLAM-blind or CD46-blind are indicated by an *asterisk* (*) or a *hash mark* (#), respectively.

One mutant, I194S (*asterisk* in Fig. 1*C*, *top line*), completely lost SLAM-dependent fusion function while fully retaining CD46-dependent fusion capacity. Three mutants (L321S, I435S and L470S; *hash mark* in Fig. 1*C*, *second* and *third line*) lost CD46-dependent fusion capacity, while retaining SLAM-dependent fusion-support. In addition, one mutant, Y543A, had a

partially impaired CD46-dependent fusion-support capacity. The block mutants, YG228–229AA and NY274–275AA completely lost receptor-dependent fusion capacity in both CHO-SLAM and Vero cells and were eliminated from further analysis. Thus, of the 64 H-protein mutants screened, five mutants identified receptor-specific fusion-support residues (1 SLAM-specific and 4 CD46-specific residues).

The Slightly Smaller Aliphatic Amino Acid Valine Functionally Substitutes Ile-194 in a Fusion-support Assay—To further characterize the role of residue 194 in SLAM-dependent fusion-support, different mutations were made. Table 1 lists these substitutions and presents the results of the SLAM- and CD46-dependent fusion assays. While radical substitutions, such as aromatic or charged amino acids, completely abolished SLAM-dependent fusion (Table 1, rows 6–9), certain conservative changes also dramatically inhibited SLAM-dependent fusion (Table 1, rows 3–5). For example leucine, different from isoleucine only in the position of a branched hydrocarbon side chain, is only 30% as efficient as the unmodified H-protein. Moreover, alanine, the smallest aliphatic amino acid also caused a similar decrease in fusion efficiency. On the other hand valine, differing from isoleucine only because of the absence of the delta methyl group, was the only amino acid that retained full SLAM-dependent fusion efficiency. Remarkably threonine, differing from valine only because it carries a hydroxyl group in place of the methyl groups on the β carbon, also strongly inhibited SLAM-dependent fusion. None of the substitutions had any effect on CD46-dependent fusion as determined using Vero cells (Table 1, *right column*). Taken together, the data indicate that Ile-194 is important for SLAM-dependent fusion and that only mutants to valine fully retain SLAM-dependent fusion-support capacity.

TABLE 1
Fusion capacity of H-proteins with mutations at position 194

Amino acid	CHO-SLAM[a] (SLAM+)	Vero[a] (CD46+)
Isoleucine	+++	+++
Valine	+++	+++
Leucine	+	+++
Alanine	+	+++
Threonine	+	+++
Serine	0	+++
Tryptophan	0	+++
Aspartic acid	0	+++
Lysine	0	+++

[a] Fusion capacity quantified as described under "Experimental Procedures."

Ile-194 Is Critical for SLAM-dependent Entry of Virus Particles—To characterize the role of Ile-194 in SLAM-dependent MV entry, viruses with different mutations of this residue were sought. The I194S, I194A, I194L, and I194T mutations were transferred to an infectious MV genome that expresses the reporter gene, green fluorescent protein, from an additional transcription unit (20). Their titers were equivalent to those of the parental virus in the CD46-expressing Vero cells. Their infectivity was then assayed in two cell lines that express SLAM, but not CD46, CHO-SLAM, and B95a. As a control, Vero cells expressing only CD46 were used.

Fig. 2 illustrates the infection of the standard and the four mutant viruses in B95a (*top row*), CHO-SLAM (*middle row*), and Vero cells (*bottom row*) 36 h after infection at an MOI of 0.1. MV containing the unmodified H-protein gives rise to large syncytia on all three cell lines. However, Ser at the 194 position, an amino acid that fully blocks SLAM-dependent fusion, also blocked infection of the two SLAM-expressing cell lines while having no effect on the infectivity of the same virus on CD46-expressing cells. Moreover, Ile-194 mutations to Ala, Leu, and Thr, partially interfering with SLAM-dependent fusion, also strongly interfered with infectivity of the corresponding viruses in SLAM-expressing cells. Thus, the mutations at Ile-194 have equivalent effects on SLAM-dependent cell-cell fusion and SLAM-dependent entry of recombinant viruses.

I194S, but Not the Quartet of Mutations in β-Sheet 5, Ablate Binding to Soluble SLAM—The assay we used identifies residues that have selective effects on CD46- or SLAM-dependent fusion, but cannot discriminate between residues involved in primary receptor binding, and those sustaining H-protein conformational changes subsequent to binding.

To assess which of these mutations has a direct effect on binding, we measured the binding kinetics of soluble forms of relevant H-protein mutants to the MV receptors by SPR in a BIAcore 3000 instrument. Toward this, soluble FLAG-tagged forms of the H-protein ectodomain (*sH*, Fig. 3*A*) were expressed and purified, including that of the vaccine strain Edmonston (sH_{NSe}), four derivatives mutated at the 194 position (sH_{I194S}, sH_{I194A}, sH_{I194L}, sH_{I194T}), and one derivative with mutations of the four bs-5 quartet amino acids ($sH_{bs5quartet}$). The sH-protein of the MV wild-type strain IC-B containing an N481Y substitution ($sH_{ICB(N481Y)}$) shown to be important for CD46 interaction was also expressed and purified.

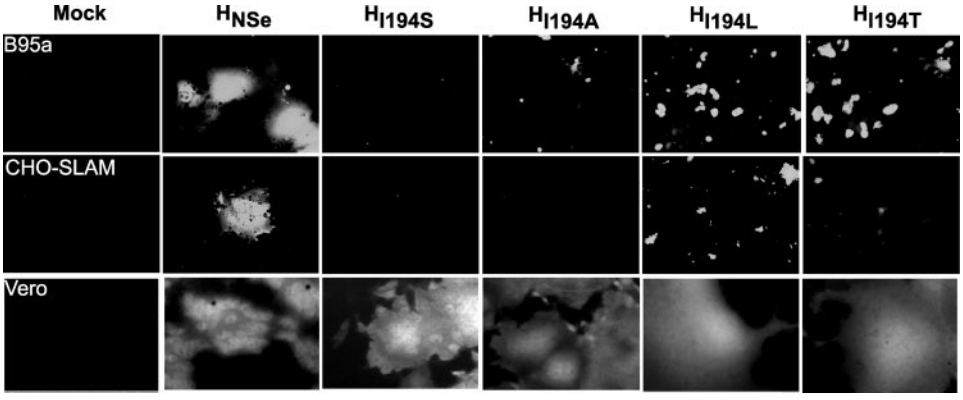

FIGURE 2. **Substitutions of Ile-194 selectively impact SLAM-dependent cell entry.** Infection of B95a, CHO-SLAM, and Vero cells with recombinant viruses carrying different substitutions at Ile-194. The *green* fluorescence emission of cells infected with the different viruses is shown.

To determine kinetics of receptor binding to sH, soluble forms of the MV receptors, SLAM or CD46, were expressed and purified. The soluble form of CD46 (sCD46) comprised the first 303 amino acids (complement control protein motifs 1–4) and soluble SLAM (sSLAM) comprised the complete extracellular domain. Multiple cycles of receptor association and

dissociation were performed using receptor concentrations ranging from 0.1 to 1 μM (Fig. 3*B*, color coding as in *inset legend*). The *top row* of panels represents the binding kinetics of the unmodified vaccine strain sH (sH_{NSe}) with sSLAM (*left*) and sCD46 (*right*). The binding kinetics of the sH-protein with the four bs-5 residues mutated ($sH_{bs5quartet}$) and that of the sH-protein with the I194S substitution (sH_{I194S}) with the sSLAM and sCD46 receptors are shown in the second and third row of panels, respectively. Both sH_{NSe} and $sH_{bs5quartet}$ exhibit a specific interaction with sSLAM (*left panel*) that increased with receptor concentration. In contrast, sH_{I194S} showed no interaction with sSLAM even at the highest receptor concentration (*bottom panel*). sH_{NSe}-, $sH_{bs5quartet}$-, and sH_{I194S}-proteins all showed equivalent interaction profiles with the sCD46 receptor, indicating their functional integrity.

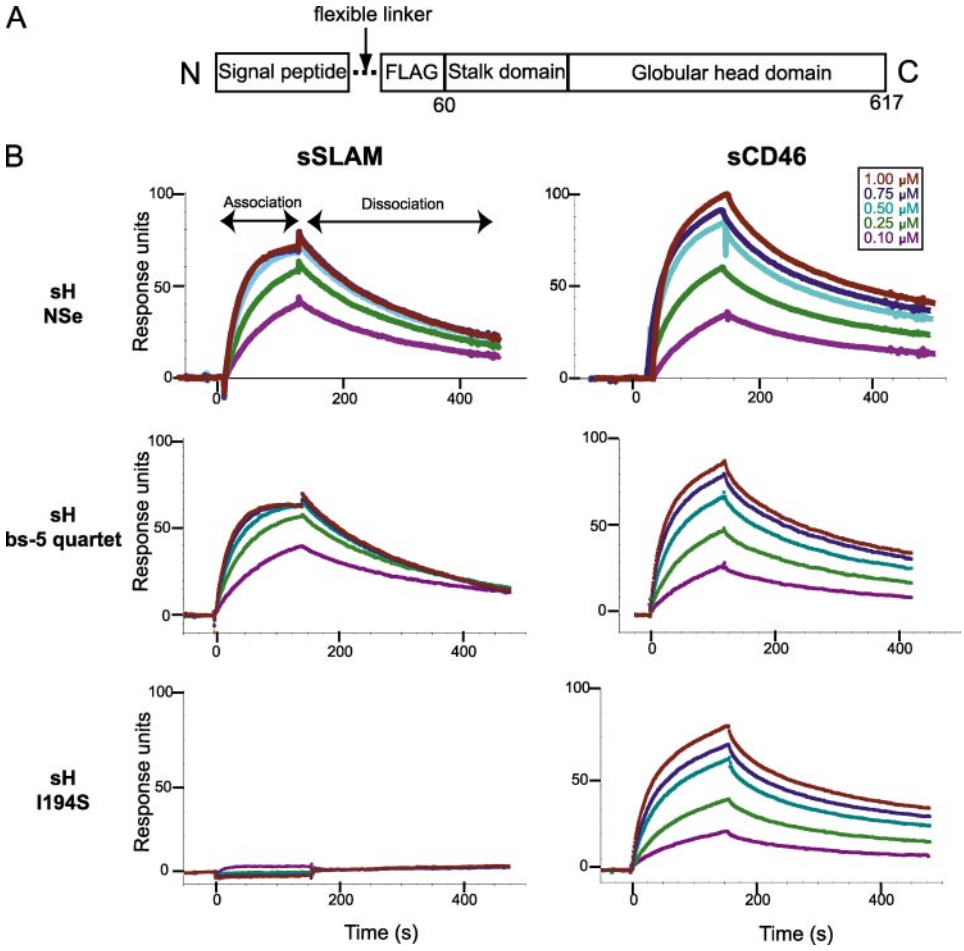

FIGURE 3. **Interaction between the soluble forms of the H-protein and its receptors SLAM and CD46 measured by SPR.** *A*, line drawing of the soluble H-protein structure. A signal peptide and a FLAG tag precede the H-protein ectodomain. The signal peptide allows secretion of the protein, and the FLAG tag allows antibody capture in the BIAcore experiments. *B*, SPR (BIAcore) sensorgrams recording the interaction, shown in resonance units over time (*s*), between sH-proteins and the soluble receptors, sSLAM or sCD46. Cycles of receptor association and dissociation performed at five different receptor concentrations are shown. The receptor concentrations used are color-coded as indicated in the *upper right corner*.

H-proteins with Conservative Ile-194 Mutations Have >1000 Times Reduced Affinity for sSLAM—The kinetic rate constants of the sH-MV receptor binding interactions determined from the sensorgrams in Fig. 3*B* are presented in Table 2, together with those for the binding of four additional mutant proteins, sH_{I194A}, sH_{I194L}, sH_{I194T}, and $sH_{ICB(N481Y)}$. A comparison of the dissociation constants (K_d) between the different sH variants and sSLAM, shows that sH_{NSe} and $sH_{bs5quartet}$ have similar affinities for SLAM (80 and 67 nM, respectively). In contrast, the dissociation constant for the interaction between sH_{I194S} and sSLAM is ~2000 times higher, indicating no appreciable binding. This result explains the lack of infectivity of the virus carrying the I194S mutation in SLAM-expressing, CD46-negative cell lines.

Moreover, sH_{I194A}, sH_{I194L}, and sH_{I194T} all have K_d values more than

TABLE 2
Affinity and kinetic rate constants for receptor binding to H-protein

MV H	sCD46[a]				sSLAM[a]			
	K_d[b]	k_{on}[c]	k_{off}[d]	Chi²[e]	K_d[b]	k_{on}[c]	k_{off}[d]	Chi²[e]
	nM	$M^{-1}s^{-1} \times 10^4$	$s^{-1} \times 10^{-3}$		nM	$M^{-1}s^{-1} \times 10^4$	$s^{-1} \times 10^{-3}$	
H_{NSe}	79	2.70	2.10	5.1	80	2.50	2.00	1.1
H_{I194S}	149	1.70	2.50	4.8	137000	NA[f]	NA	0.7
H_{I194A}	132	3.00	3.90	6.2	171000	NA	NA	0.9
H_{I194L}	137	2.30	3.20	9.9	147000	NA	NA	1.7
H_{I194T}	65	5.80	3.80	3.8	83600	NA	NA	0.2
$H_{bs\text{-}5\ quartet}$[g]	97	3.28	3.20	2.7	67	7.50	4.90	4.3
$H_{ICB(N481Y)}$	1460	NA	NA	0.5	47	3.10	1.40	0.4

[a] Interaction between soluble H variants and the soluble receptors sCD46 and sSLAM were measured with a BIACORE 3000 instrument and fit using the 1:1 Langmuir binding model.
[b] The dissociation constant for the interaction (nanomolar).
[c] The association rate constant (per mol per second).
[d] The dissociation rate constant (per second).
[e] The root mean square deviation of the fitted curve from the experimental curve. Values below 10 are considered acceptable.
[f] NA, not applicable.
[g] Y529A, D530A, R533A, and Y553A.

1000 times higher than that of sH_{NSe}, indicating that Ile-194 is critical for H-protein binding to SLAM. The fact that the K_d for the CD46 interaction only doubled for these proteins confirms that this effect is SLAM-specific, and indicates that the mutation did not compromise the overall structure of the mutant H-proteins. These kinetic data indicate that the I194S mutation affects receptor binding whereas the bs-5 quartet mutations may affect a post-binding event.

The affinity between H and SLAM reported in our study is up to five times stronger than that reported previously (80 *versus* 400 nM) (29, 30). The stronger association we observe between H and SLAM as compared with these previous studies may be explained by the fact that we used a sH construct which comprised the complete H ectodomain (residues 60–617) as opposed to a truncated form (residues 149–617).

N481Y Enables Wild-type H-protein to Bind sCD46—We also report the binding kinetics of sH-protein from the IC-B wild-type strain of MV. The N481Y substitution, known to be important for CD46-dependent fusion, was introduced into this protein. $sH_{ICB(N481Y)}$, and sH_{NSe} have similar affinities for sSLAM (K_d values of 47 *versus* 80 nM, respectively). In contrast, the wild-type strain H-protein has a significantly lower affinity for sCD46 compared with that of sH_{NSe} (K_d values of 1460 nM *versus* 79 nM, respectively). A recent analysis of the binding kinetics of sH_{ICB} did not detect an interaction between sCD46 and the wild-type H-protein (30). Thus, the N481Y mutation increases the affinity between the wild-type H-protein and the CD46 receptor. However, the affinity is ~18 times lower than that seen for sH_{NSe}, indicating that other mutations are necessary to fully explain the ability of the MV vaccine strain to use CD46 as a receptor. This result is consistent with a previous study where a recombinant MV clinical isolate carrying the N481Y substitution was generated and found to infect CD46-positive, SLAM-negative cells inefficiently (31).

Viruses with an I194S H-protein Bind Inefficiently to SLAM-expressing Cells—The biochemical analysis of sH binding to the MV receptors failed to detect a sH_{I194S}-sSLAM interaction. To study the effect of this mutation on MV binding to SLAM-positive, CD46-negative cells, we quantified the amount of virus bound to B95a cells by FACS. B95a cells were incubated with an equal number of purified H_{NSe}- or H_{I194S}-containing virus particles (MV_{NSe} and MV_{I194S}, respectively), as determined by densitometric analysis of a Western blot of the purified viruses (Fig. 4, *inset*). Any unbound virus was washed away, the virus detected with a monoclonal anti-H antibody, and the cell-bound virus quantified by FACS analysis. The *filled curve* in Fig. 4 represents the negative control with no virus bound. When MV_{NSe} is incubated with B95a cells, a substantial increase in the fluorescence signal is recorded (mean fluorescence intensity = 147). When the same amount of MV_{I194S} was incubated with the B95a cells, the increase in the signal was less pronounced (mean fluorescence intensity = 58), indicating that the I194S mutation partially interferes with virus-cell binding. However, MV_{I194S} bound to B95a cells with about 40% efficiency as parental virus, whereas H_{I194S} binding to sSLAM was about 1000 times less efficient. It should be noted that similar results were observed with another SLAM-expressing cell line, CHO-SLAM. It is possible that the virus binds to other cell surface proteins, but these interactions are minimally productive (32).

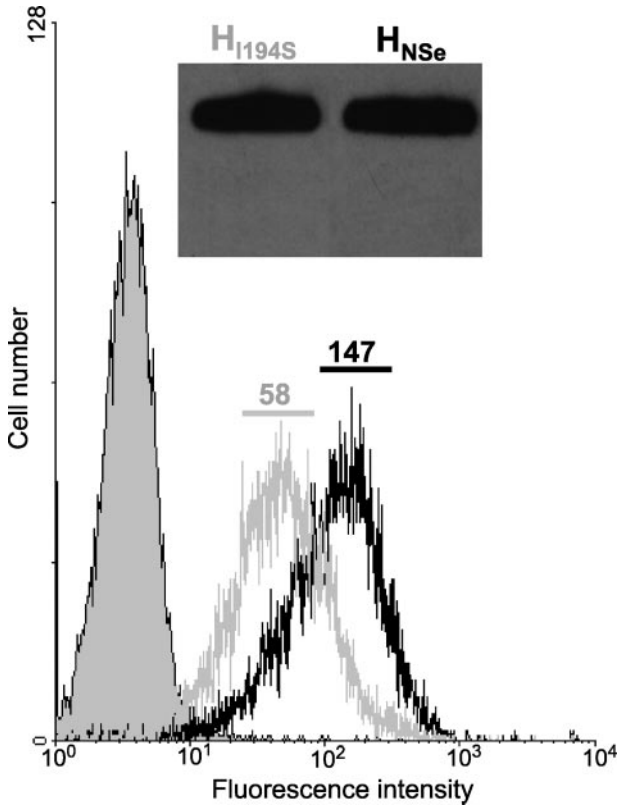

FIGURE 4. **Virus binding to cells.** Virus particles were purified on a sucrose gradient, and the virus fraction was analyzed by Western blot (*inset*; an anti-H antibody was used). An equal number of particles of H_{NSe} (*black line*) or H_{I194S} (*gray line*) (as determined by densitometry) were incubated with 2×10^5 B95a cells. Virus was detected with an anti-H monoclonal antibody and a PE-conjugated secondary antibody. Mean fluorescence intensity is indicated above the curve. *Filled curve*, control cells without virus.

DISCUSSION

A model-based approach predicting MV H-protein residues potentially involved in protein-protein interactions guided mutagenesis that identified Ile-194 as a critical residue for SLAM-dependent fusion. Receptor binding studies showed that Ile-194 is involved in primary SLAM-binding, while the bs-5 quartet mutations (Tyr-529, Asp-530, Arg-533, and Tyr-553) support a post-binding step necessary to elicit F-protein unfolding and membrane fusion.

The location of these residues is visualized in Fig. 5 on the recently published crystal structure of the H-protein ectodomain dimer (30). In this structure the two H monomers tilt oppositely toward the horizontal plane. This orients propeller blades 5 and 6 with the SLAM-relevant residues upwards toward the target cell (Fig. 5, *A* and *B*; SLAM relevant residues are colored *red*, *orange*, or *yellow*). Fig. 5*A* (*top view* of homodimer) identifies Ile-194, Asp-505, Asp-507, Tyr-529, Asp-530, Thr-531, Arg-533, His-536, Tyr-553, and Pro-554 as at least in part solvent-accessible. These SLAM-relevant residues define a binding site on the top of the H-protein homodimer.

We note that these residues have been defined as SLAM-relevant based on different assays. As discussed, Ile-194, Tyr-

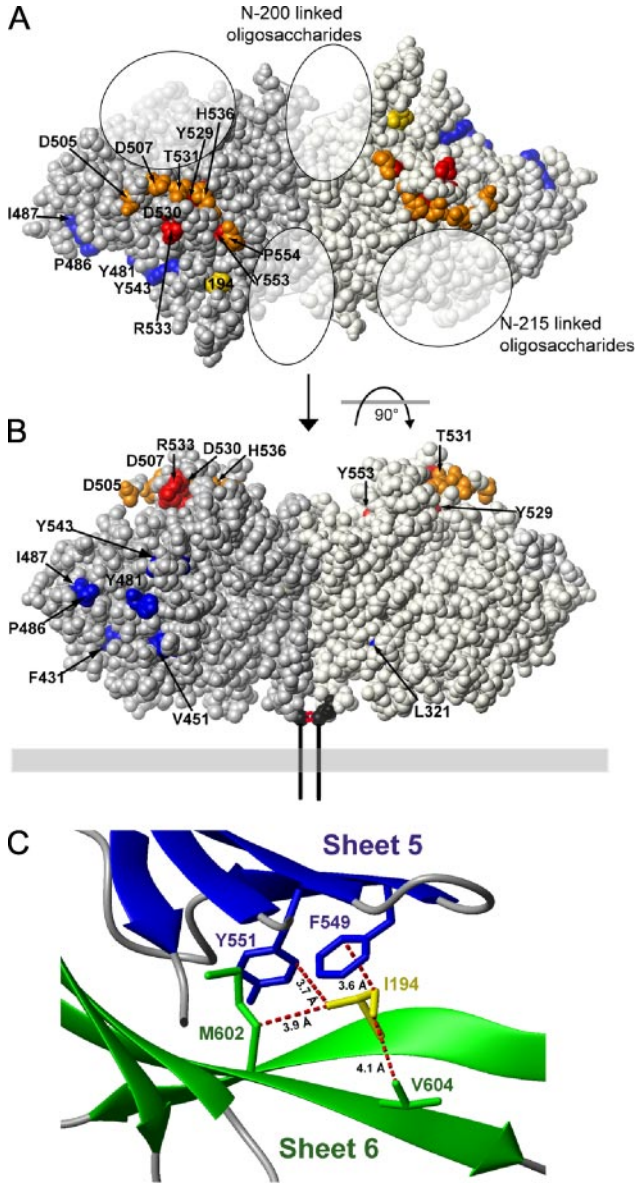

FIGURE 5. **Residues important for SLAM- or CD46-dependent entry.** *A*, top view of the crystal structure of the MV H homodimer depicted as a *space-filling model*. The two H-protein monomers are shaded in *gray* (*left*) and *light gray* (*right*) for clarity. Residues colored *red* are necessary for SLAM-dependent entry but are not involved in primary binding to the receptor. Ile-194 colored *yellow* is necessary for SLAM-dependent entry and primary binding. Residues colored *orange* are SLAM-dependent fusion-support residues with undetermined function. CD46-dependent fusion-support residues are colored *blue*. *B*, side view of the homodimer generated by rotating the *top view* depicted in *A* by 90° around the *x*-axis. Residue Cys-154, the anchor residue of the stalk region, is colored *black*. Two *red lines* represent the C154-C154 disulfide bond that links the two monomers in the homodimer. Residues 1–153, not present in the crystal structure and comprising the cytoplasmic tail, transmembrane, and stalk regions are represented as a *vertical black line*. The membrane is illustrated as a *horizontal gray box*. *C*, interactions of Ile-194 with neighboring MV H residues. Closest distances between heavy atoms of Ile-194, and interaction partners are depicted as *dotted red lines*. Ile-194 has van der Waals contacts with Tyr-551 and Phe-549 on sheet 5 (in *blue*) and with Met-602 and Val-604 on sheet 6 (in *green*).

529, Asp-530, Thr-531, Arg-533, Tyr-553, and Pro-554 were identified based on a receptor-dependent fusion assay (15). Asp-505, Asp-507, and His-536 were initially shown only to significantly reduce SLAM-down-regulation (33). We have subsequently tested D505G and D507G mutations in a receptor-specific cell-to-cell fusion assay and confirmed that they cause a two-third decrease in SLAM-dependent fusion (data not shown).

Residues identified by the functional assays discussed above may sustain receptor binding or subsequent receptor-specific H-protein conformational changes. Remarkably, in the H-protein conformation that formed crystals, only 15% of the Ile-194 surface is solvent-exposed and available for binding (Fig. 5*A*, *yellow residue*). Comparatively, Tyr-529, Tyr-553, Asp-530, and Arg-533 (bs-5 quartet residues; Fig. 5, *A* and *B*, *red residues*) have 1, 4, 10, and 33% of their surfaces accessible to solvent, respectively. Thus, most of the bs-5 quartet residues are minimally accessible to cellular receptors, an observation consistent with their lack of binding function. However, they may take part in subsequent conformational changes required for fusion activation.

Attempts to modulate sH-protein binding to sSLAM by exchanging the side chain of the 194 position were unsuccessful, as all substitutions resulted in a greater that 1000-fold increase in the K_d, indicating complete loss of binding. However, the membrane protein-based fusion assays indicated that residues with certain side chains maintained function, and measured significant differences in the fusion-support efficacy of different side chains. While Ser completely abolished fusion-helper function and infectivity in SLAM-positive cells, Ala, Leu, and Thr conducted some fusion-support function (Table 1) and infectivity (Fig. 2). A comparison of the amino acids that maintain function and those that lose it reveal branched methyl groups at the β-carbon as a common feature of functional amino acids. If not directly involved in SLAM-binding, this feature must sustain a protein conformation allowing it (see below).

The identity of residue 481 determines the ability of MV H to use CD46 as a receptor: H-proteins from MV wild-type strains have Asn at this position while vaccine strains have Tyr (10, 28, 31). Based on SPR binding analysis, Hashiguchi *et al.* (2007) reported that the wild-type strain (IC-B) H-protein does not bind to CD46. We tested the binding kinetics of sH_{ICB} carrying the N481Y mutation and recorded a K_d of 1460 nM, an affinity similar to that seen between cell adhesion molecules (34). Thus, the single Tyr substitution at 481 confers on the H-protein the ability to bind CD46, where previously it had no interaction.

Regarding the interaction with SLAM, we have documented that certain membrane-bound H-protein mutants maintain considerable cell-binding and membrane fusion-support function, while the SLAM-binding efficiency of the corresponding soluble protein ectodomains decreases 1000 times. Binding to cell surface proteins other than SLAM may account for part of this effect. In addition, membrane-bound H may be more conducive to receptor binding, possibly because it is more dynamic than its soluble ectodomain (see below). Alternatively, the H-protein membrane-bound form may be constrained in an intermediate conformation more conducive to SLAM binding than the ectodomain alone.

Our analysis of the H-protein interaction with SLAM reveals that it is based on sequential H-protein conformational changes. The initial SLAM interaction is influenced by Ile-194. Fig. 5*C* illustrates how this residue, located on one β-strand of

propeller blade 6 (*green color*), engages in van der Waals interactions (*red interrupted lines*) with Met-602 and Val-604 on another β-strand of propeller blade 6, as well as with Phe-549 and Tyr-551 on a β-strand of propeller blade 5 (*blue color*), stabilizing this interface. Because only 15% of the Ile-194 surface is solvent-exposed, destabilization of this interface explains the effects of residue 194 mutations better than direct receptor binding. We note that the available H-protein crystal structure only represents one of its possible conformations. On the other hand, the binding and fusion assays are based on H-proteins whose propeller blades and amino acid side chains are constantly moving in solution as a result of thermal energy (35). Thus, SLAM may bind to only one of the many conformations that H continually samples, and substitutions at residue 194 may preclude the generation of an H-protein conformation conducive to primary binding. We are probing the H-protein with conformation-dependent antibodies to identify structural changes as a result of Ile-194 substitutions.

Remarkably, none of the four residues initially identified as essential for SLAM-dependent fusion-support affects SLAM-binding (15). This proves that not only binding, but also subsequent H-protein conformational changes can be receptor-specific. It also implies that alternative pathways of H-protein conformational changes can converge to trigger F-protein unfolding and membrane fusion (12). In retrospect, the fact that many different specificity domains displayed on the H-protein can elicit fusion through targeted receptors (36–38) can be rationalized by the availability of alternative pathways of H-protein conformational changes eliciting membrane fusion.

In summary, our results and the MV H crystal structure (30) set the stage for the atomic level characterization of the dynamics of H-protein-receptor interactions. Analogous processes may operate during membrane fusion relying on the envelope glycoproteins of other genera of the *Paramyxoviridae* family.

Acknowledgments—We thank Patricia Devaux, Vincent Leonard, Jorge Reyes Del Valle, and Andrew Hudacek for help and for reading the manuscript, and Hannah Koble for secretarial assistance.

REFERENCES

1. Strebel, P. M., Papania, M. J., and Halsey, N. A. (2004) in *Vaccines* (Plotkin, S. A., and Orenstein, W. A., eds), Ed. 4, pp. 389–440, Saunders-Elsevier, Philadelphia, PA
2. Borrow, P., and Oldstone, M. B. (1995) *Curr. Top Microbiol. Immunol.* **191,** 85–100
3. Duclos, P., and Ward, B. J. (1998) *Drug Saf.* **19,** 435–454
4. Tatsuo, H., Ono, N., Tanaka, K., and Yanagi, Y. (2000) *Nature* **406,** 893–897
5. Ono, N., Tatsuo, H., Hidaka, Y., Aoki, T., Minagawa, H., and Yanagi, Y. (2001) *J. Virol.* **75,** 4399–4401
6. Hsu, E. C., Iorio, C., Sarangi, F., Khine, A. A., and Richardson, C. D. (2001) *Virology* **279,** 9–21
7. Erlenhoefer, C., Wurzer, W. J., Loffler, S., Schneider-Schaulies, S., ter Meulen, V., and Schneider-Schaulies, J. (2001) *J. Virol.* **75,** 4499–4505
8. Naniche, D., Varior-Krishnan, G., Cervoni, F., Wild, T. F., Rossi, B., Rabourdin-Combe, C., and Gerlier, D. (1993) *J. Virol.* **67,** 6025–6032
9. Dorig, R. E., Marcil, A., Chopra, A., and Richardson, C. D. (1993) *Cell* **75,** 295–305
10. Schneider, U., von Messling, V., Devaux, P., and Cattaneo, R. (2002) *J. Virol.* **76,** 7460–7467
11. Cattaneo, R., and Rose, J. K. (1993) *J. Virol.* **67,** 1493–1502
12. Yin, H. S., Wen, X., Paterson, R. G., Lamb, R. A., and Jardetzky, T. S. (2006) *Nature* **439,** 38–44
13. Plemper, R. K., Hammond, A. L., and Cattaneo, R. (2000) *J. Virol.* **74,** 6485–6493
14. Crennell, S., Takimoto, T., Portner, A., and Taylor, G. (2000) *Nat. Struct. Biol.* **7,** 1068–1074
15. Vongpunsawad, S., Oezgun, N., Braun, W., and Cattaneo, R. (2004) *J. Virol.* **78,** 302–313
16. Negi, S. S., and Braun, W. (2007) *J. Mol. Model* **13,** 1157–1167
17. Radecke, F., Spielhofer, P., Schneider, H., Kaelin, K., Huber, M., Dotsch, C., Christiansen, G., and Billeter, M. A. (1995) *EMBO J.* **14,** 5773–5784
18. Negi, S. S., Schein, C. H., Oezguen, N., Power, T. D., and Braun, W. (2007) *Bioinformatics* **23,** 3397–3399
19. Cathomen, T., Buchholz, C. J., Spielhofer, P., and Cattaneo, R. (1995) *Virology* **214,** 628–632
20. Duprex, W. P., McQuaid, S., Hangartner, L., Billeter, M. A., and Rima, B. K. (1999) *J. Virol.* **73,** 9568–9575
21. Rager, M., Vongpunsawad, S., Duprex, W. P., and Cattaneo, R. (2002) *EMBO J.* **21,** 2364–2372
22. Holmen, S. L., Salter, D. W., Payne, W. S., Dodgson, J. B., Hughes, S. H., and Federspiel, M. J. (1999) *J. Virol.* **73,** 10051–10060
23. Kumar, R., and Stanley, P. (1989) *Mol. Cell. Biol.* **9,** 5713–5717
24. Negi, S. S., Kolokoltsov, A. A., Schein, C. H., Davey, R. A., and Braun, W. (2006) *J. Mol. Model* **12,** 921–929
25. Schein, C. H., Zhou, B., and Braun, W. (2005) *Virol J.* **2,** 40
26. Bartz, R., Brinckmann, U., Dunster, L. M., Rima, B., ter Meulen, V., and Schneider-Schaulies, J. (1996) *Virology* **224,** 334–337
27. Hsu, E. C., Sarangi, F., Iorio, C., Sidhu, M. S., Udem, S. A., Dillehay, D. L., Xu, W., Rota, P. A., Bellini, W. J., and Richardson, C. D. (1998) *J. Virol.* **72,** 2905–2916
28. Lecouturier, V., Fayolle, J., Caballero, M., Carabana, J., Celma, M. L., Fernandez-Munoz, R., Wild, T. F., and Buckland, R. (1996) *J. Virol.* **70,** 4200–4204
29. Santiago, C., Bjorling, E., Stehle, T., and Casasnovas, J. M. (2002) *J. Biol. Chem.* **277,** 32294–32301
30. Hashiguchi, T., Kajikawa, M., Maita, N., Takeda, M., Kuroki, K., Sasaki, K., Kohda, D., Yanagi, Y., and Maenaka, K. (2007) *Proc. Natl. Acad. Sci. U. S. A.* **104,** 19535–19540
31. Seki, F., Takeda, M., Minagawa, H., and Yanagi, Y. (2006) *J. Gen. Virol.* **87,** 1643–1648
32. Hashimoto, K., Ono, N., Tatsuo, H., Minagawa, H., Takeda, M., Takeuchi, K., and Yanagi, Y. (2002) *J. Virol.* **76,** 6743–6749
33. Masse, N., Ainouze, M., Neel, B., Wild, T. F., Buckland, R., and Langedijk, J. P. (2004) *J. Virol.* **78,** 9051–9063
34. Simonis, D., Christ, K., Alban, S., and Bendas, G. (2007) *Semin. Thromb. Hemost.* **33,** 534–539
35. Henzler-Wildman, K., and Kern, D. (2007) *Nature* **450,** 964–972
36. Schneider, U., Bullough, F., Vongpunsawad, S., Russell, S. J., and Cattaneo, R. (2000) *J. Virol.* **74,** 9928–9936
37. Nakamura, T., Peng, K. W., Harvey, M., Greiner, S., Lorimer, I. A., James, C. D., and Russell, S. J. (2005) *Nat. Biotechnol.* **23,** 209–214
38. Ungerechts, G., Springfeld, C., Frenzke, M. E., Lampe, J., Johnston, P. B., Parker, W. B., Sorscher, E. J., and Cattaneo, R. (2007) *Cancer Res.* **67,** 10939–10947